

Hierarchically Structured Millimeter-Sized (Organo) Silica Spheres with a Macroporous Shell and a Meso/Microporous Core

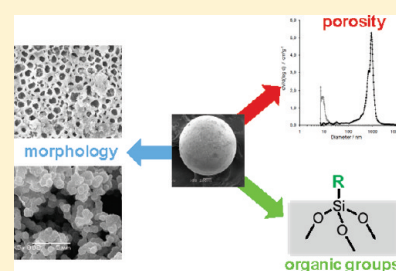
Sabine Scholz and Johannes A. Lercher*

Technische Universität München, Department of Chemistry, Catalysis Research Center, Institut für Siliciumchemie, Lichtenbergstrasse 4, 85747 Garching, Germany

S Supporting Information

ABSTRACT: Tailored hierarchically structured (organo) silica beads with particle diameters between 0.3 and 2.5 mm have been prepared using an emulsion based sol–gel approach. Poly(propylene oxide)-poly(ethylene oxide) triblock copolymers as surfactants, aniline or 1-butanol as solvent and different silanes such as tetraethyl silicate, [3-(2-aminoethylamino)propyl]trimethoxysilane and phenyltrimethoxysilane are used to direct morphology and porosity. The silica spheres provide specific surface areas up to 900 m²/g and adjustable porosity in the meso- and macroporous region. The texture includes particulate structures with controllable size between 80 nm and 2.5 μm of the silica particles on the inside of the spheres and a macroporous foam-like shell with macropores in the range between 0.2 and 4.0 μm and a thickness of the shell between 0.6 and 44 μm. The high variability of this preparation method and the simultaneous control of the nano- to millimeter scale structure including the porosity as well as the morphology allows one to design tailor-made adsorbents and catalysts.

KEYWORDS: tunable millimeter sized (organo) silica spheres, hierarchical structure, macroporous shell, meso/microporous core, emulsion-based sol–gel synthesis



1. INTRODUCTION

Mesoporous materials with tunable properties are of great interest in many fields of applications including catalyst supports and adsorbents. For such applications, it is important to adjust the morphology and shape of the materials (in addition to the pore sizes) in order to optimize the mass transport.¹ The simultaneous control of the nano-, micro-, and macroscale properties of porous materials during synthesis is challenging, but would allow for a unique and time-economic approach toward synthesis.

For the preparation of spherical mesoporous particles, different preparation pathways have been proposed. The three most typical ones are based on a biphasic emulsion system,² on the controlled hydrolysis by combination of the Stöber synthesis with mesophase formation^{3,4} and on spray-drying of sol droplets.⁵ The limitations of these procedures are related to the fact that only particles in the nano- and micrometer range with a relatively broad particle size distribution and agglomerates of these particles are usually obtained. The first uniform macroscopic silica spheres with a controllable diameter from 0.1–2 mm and pore sizes between 1 and 5 nm were prepared by Stucky et al.⁶ The spheres were synthesized using an oil-in-water emulsion approach by adding tetrabutyl orthosilicate (TBOS) to a solution of the cationic surfactant cetyltrimethylammonium bromide (CTAB) in water and NaOH and stirring this mixture for 15–30 h.

This allowed the control of shape and porosity on two different length scales and induced a large number of studies on bi- and multiple phase systems. Most of these are focused on the synthesis of materials with larger mesopores and especially on the preparation of hierarchical mesoporous-macroporous materials.⁷

Meso- and macro-cellular silica foams were synthesized by an acid catalyzed gelation of a tetraethyl orthosilicate (TEOS)–mesitylene mixture, which was slowly added to an aqueous CTAB solution.⁸ A macroporous silica monolith with vermicular-type mesostructure has been prepared by a time-consuming emulsion-based addition of dodecane to an acidic sol of TEOS and tetradecyltrimethylammonium bromide (TTAB).⁹ Another possible route used double templating and a multiple emulsion system (O₁/W/O₂) with different surfactants such as Tween 20, Span 80, polyethylene glycol, or hydroxypropyl cellulose and organic solvents such as n-hexane and n-decyl alcohol.¹⁰ This complex system allowed the synthesis of spherical nanoparticles. Because of the metastability of the emulsions, such a strategy may lead to problems for syntheses on longer time scales, and methods relying on shorter formation times would be preferable.

To address this, we carried out the preparation of hierarchically structured silica spheres explored in this paper in a continuously operated reactor column with a recycling heated water flow via hydrolysis and condensation of silicon alkoxides, which is known to be a mild and versatile reaction approach. The system provides high reproducibility of the synthesis and a narrow size distribution of the silica spheres.¹¹ The hydrolysis and condensation of the silanes is initiated by injection of the precursor solution containing different silanes and a surfactant, which are dissolved in 1-butanol or aniline, into the reactor column. This leads to a surfactant stabilized oil-in-water

Received: November 17, 2010

Revised: March 13, 2011

Published: March 29, 2011

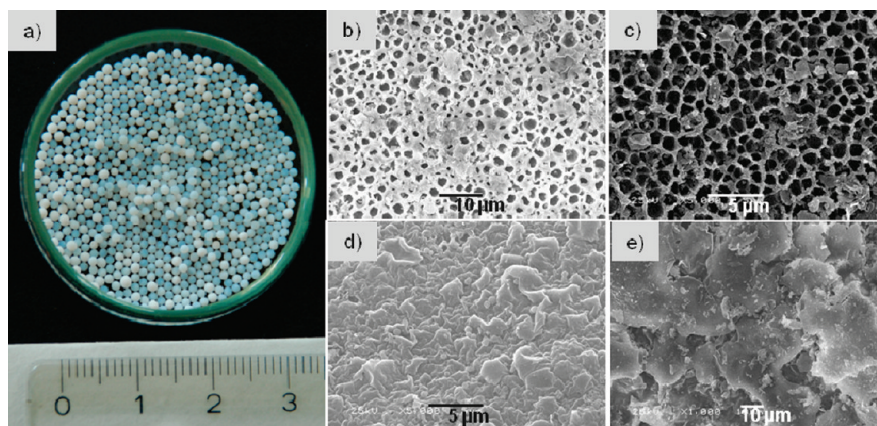


Figure 1. Morphology of calcined silica spheres made with different surfactants. Photograph of (a) calcined silica spheres and SEM images of the sphere surface with increasing hydrophobicity of the surfactant (b) $(\text{PO})_{18}(\text{EO})_{45}(\text{PO})_{18}$ (Pluronic 25R4), (c) $(\text{PO})_{11}(\text{EO})_{27}(\text{PO})_{11}$ (Pluronic RPE 1740), (d) $(\text{PO})_{13}(\text{EO})_{16}(\text{PO})_{13}$ (Pluronic RPE 1720), and (e) $(\text{PO})_{27}(\text{EO})_6(\text{PO})_{27}$ (Pluronic RPE 3110).

emulsion, which hydrolyzes first on the outside forming a shell-like structure through which, the water diffuses and eventually causes complete hydrolysis and condensation. The advantage of this approach compared to other silicon alkoxide emulsion systems is that the precursor solution contains all the relevant chemicals and that the continuous phase consists only of water.^{6,10}

In the present contribution we explore, therefore, how by choice of surfactant, solvent, and silanes, the structure and the properties of macroscopic silica spheres can be manipulated to design materials as catalyst supports or sorbents. The target is to present and provide a knowledge-based tool box for the preparation of (functionalized) tailor-made macroscopic silica spheres.

2. EXPERIMENTAL SECTION

2.1. Materials. Tetraethyl silicate (TES40), N-cyclohexyl-3-amino-propyltrimethoxysilane (GF92), N-phenylaminomethyltrimethoxysilane (XL973), N-cyclohexylaminomethylmethyldiethoxysilane (XL924), N-cyclohexylaminomethyltriethoxysilane (XL926) from Wacker Chemie AG; [3-(2-aminoethylamino)propyl]trimethoxysilane (AAMS, 97%), phenyltrimethoxysilane (PTMS, 97%), aniline (99%), 1-butanol (99.9%) from Sigma Aldrich, ethanol from Merck and the surfactants Pluronic 25R4 ($\text{PO}_{18}\text{EO}_{45}\text{PO}_{18}$, $M_w = 4074$ g/mol), Pluronic RPE1740 ($\text{PO}_{11}\text{EO}_{27}\text{PO}_{11}$, $M_w = 2476$ g/mol), Pluronic RPE1720 ($\text{PO}_{13}\text{EO}_{16}\text{PO}_{13}$, $M_w = 2270$ g/mol) and Pluronic RPE3110 ($\text{PO}_{27}\text{EO}_6\text{PO}_{27}$, $M_w = 3437$ g/mol) from BASF were used in the described syntheses. All chemicals were used without further purification. The reactions were carried out with deionized water.

2.2. Synthesis of Silica Spheres. Silica composite spheres were prepared by injection of the precursor solution in a water filled reactor column (see the Supporting Information). The Pluronic triblock copolymer (14.0 g) was dissolved in 15 mL aniline under stirring. The silanes TES40 (15.50 g), PTMS (11.16 g) and AAMS (8.63 g) were mixed and added to the copolymer solution. This solution was injected via a syringe pump at 15 mL/h into the recycling water flow of the reactor column which was heated to 65 °C. The product was recovered by decantation, washed three times with water and dried under ambient conditions. The samples were calcined in air at 600 °C for 3 h with a heating rate of 1 K/min to remove the surfactant and organic moieties. The used surfactants are Pluronic 25R4, Pluronic RPE1740, Pluronic RPE1720 and Pluronic RPE3110. The variation of the surfactant concentration was carried out with Pluronic 25R4 changing the silane to surfactant weight ratios from 2.2 to 30.4. To investigate the influence of the solvent, we used a precursor solution containing 6.0 mL (5.6 g) of

TES40, 2.48 mL of AAMS, 3.16 mL of PTMS and 5.6 g of Pluronic 25R4 solved in 8.0 mL of 1-butanol (instead of aniline). The influence of the silane mixture was studied with precursor solutions containing 3.0 mL of TES40, 1.24 mL of AAMS, x mL of a sterically demanding functional silane, and 2.8 g of Pluronic 25R4 solved in 3.0 mL of aniline. The applied functional silanes are N-cyclohexyl-3-aminopropyltrimethoxysilane (GF92, $x = 2.21$ mL), N-phenylaminomethyltrimethoxysilane (XL973, $x = 1.76$ mL), N-cyclohexylaminomethyltriethoxysilane (XL926, $x = 2.46$ mL), and N-cyclohexylaminomethylmethyldiethoxysilane (XL924, $x = 2.23$ mL).

The silica composite spheres, which were used for solvent extraction, were prepared according to the described method with TES40, AAMS, PTMS, Pluronic RPE1740, and aniline. After drying at ambient conditions 1.0 g of the silica composite spheres were extracted with 300 mL of boiling ethanol for 24 h using a Soxhlet apparatus.

2.3. Characterization. The thermogravimetric analyses (TGA) of the samples were performed using a Netzsch STA 409PC Luxx instrument or TGA Q5000 V3.10 Build 258 instrument. The measurements were carried out under synthetic air with a heating rate of 5 K/min for the as-synthesized samples. The morphology was investigated with scanning electron microscopy (SEM) (JEOL JSM-5900LV). SEM images of the Au-sputtered samples (whole spheres and cross-section) were taken at acceleration voltages between 10 and 25 kV. The porosity of the products was investigated using nitrogen physisorption (Thermo Finnigan, Sorptomatic 1990 series) and mercury porosimetry (PMI Europe, Porous Materials Inc.). Prior to the measurements, the samples were degassed at 250 °C for 2 h. The specific surface area was calculated according to the BET method, the mesopores were analyzed according to the BJH and the micropores via the t-plot method.

3. RESULTS AND DISCUSSION

The described method leads to tailored hierarchically structured (organo) silica spheres with particle diameters between 0.3 and 2.5 mm via an emulsion-based sol-gel synthesis. Such particles can be functionalized and have high mechanical stability. The size and distribution of pores as well as the nano- to macroscale morphology depend subtly on the preparation parameters, which include the variation of the surfactant concentration, the role of the solvent and the modification of the silane mixture. In addition, we explored ways to remove the templates in an environmentally and economically more compatible way. These parameters can be used to adjust and tailor the properties of micrometer- to millimeter-sized organo functional silica spheres.

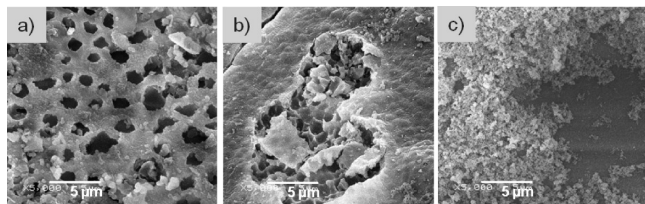


Figure 2. SEM images of the surface of silica spheres with silane to surfactant ratios of (a) 2.2, (b) 15.3, and (c) 30.4.

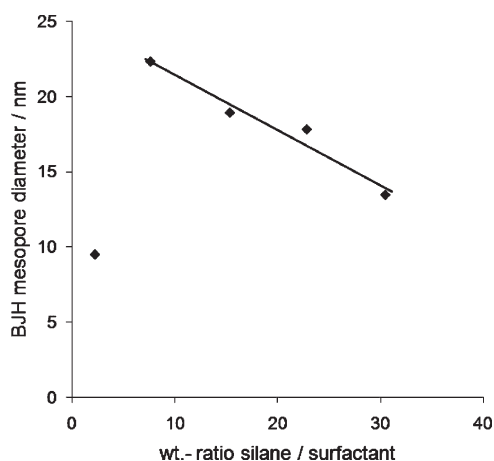


Figure 3. Dependence of the BJH mesopore diameter of calcined silica spheres on the silane to surfactant weight ratio.

3.1. Variation of the Surfactant Concentration. Especially hydrophobic amphiphilic block copolymers such as the reverse Pluronic polymers are ideally suited to stabilize an emulsion system of a precursor solution containing silanes, surfactants and a solvent in water. The polymers tend to form micelles and ordered mesophases, that allow the inducement of well-defined pores in the macroscopic silica spheres. The comparison of several triblock copolymers with varying ethylene oxide and propylene oxide chain length and molecular weights shows that the diameter of the resulting mesopores increases with increasing the hydrophobicity of the surfactant, whereas a large fraction of more hydrophilic constituents in the triblock copolymer leads to foamlike surface structures (Figure 1).

In establishing this, we noted a large impact of the surfactant concentration on the porosity as well as on the morphology of the spheres. Varying the concentration of Pluronic 25R4 relative to the amount of silanes (weight ratios from 2.2 to 30.4), mechanically stable silica spheres with a translucent milky appearance were synthesized. The precursor droplets with the lowest surfactant concentration were the least stabilized, resulting in some egg-shaped bodies. High surfactant concentrations induce the formation of a well-structured macroporous surface with pore diameters from 1 to 4 μm (see Figure 2). The reduction of the surfactant concentration causes a successive variation of the surface to less ordered structures. This is manifested by ill-developed macropores covered by a compact silica layer and an inhomogeneous surface morphology consisting of dense and particulate parts.

However, the variation of the surfactant concentration did not only influence the surface of the spheres, but also their inner structure. N_2 -adsorption shows that the mesopore diameter

decreases with decreasing concentration of the surfactant with a notable exception for the sample with the highest surfactant concentration (Figure 3). This latter material has also a larger BET surface area than the other samples. For all other samples, the BET surface area and the meso- and micropore volume practically are not affected by the concentration of the used surfactant (Table 1).

The results show that the variation of the surfactant concentration affects both the morphology of the spheres and the mesopore diameter. The surface structure of the spheres is controlled by the reactivity at the interface between the precursor droplet and the continuous water phase. The dependence on the surfactant concentration suggests that the surfactant molecules interact with the hydrophobic precursor phase as well as with the continuous water phase. This takes place via alignment of the triblock copolymer molecules along the interface according to their amphiphilic character, which results in a stabilization of the precursor droplet.¹²

The water diffusion into the precursor droplet implicates that the macroporous surface structure is formed via local phase separation. The diffusing water is speculated to cause the formation of a microemulsion consisting of water-filled micelles in the surface near layer of the precursor droplet. The highly reactive silane mixture rapidly hydrolyzes by contact with water resulting in encapsulated water droplets.¹³ After drying and calcination, only solid silica remains and the space of the encapsulated water droplets appear as macropores. Consequently, this process can only occur, if the surfactant has sufficient hydrophilicity and if the surfactant concentration is considerably higher than the critical micelle concentration (CMC). The first conclusion is supported by the variation of the sphere surface after using different surfactants (monitored by SEM analysis), i.e., the macroporous surface is only observed for surfactants with distinct hydrophilicity (see Figure 1). The second conclusion is supported by the variation of the pore structure, when reduced surfactant concentrations were used. The reduction by 80% compared to the initial concentration resulted in less pronounced macropores. The sample containing only 10% of the initial surfactant concentration completely lacked in surface macropores (see Figure 2). This last sample already indicates a destabilization of the precursor droplet due to the occurrence of some egg-shaped silica bodies.

The variation in the surfactant does not only influence the morphology of the spheres via the stabilization of the emulsion and the enhancement of the water diffusion, but also the mesopore formation. Even though the self-assembly of surfactant molecules and silica species to micelles and ordered mesophases is complex, it is nowadays quite predictable.^{14–17} The situation for the synthesis approach is here more complex, because the macroscopic silica spheres were prepared by using a biphasic system.

The crucial feature of systems with a large fraction of interfaces such as foams or emulsions is the overlap between the interfacial interaction and the microphase separation. The problem is related to the fact that the interfacial alignment reduces the accessible fraction of surfactant molecules in the bulk phase. Notably, the present results show that the mesopore diameter decreases linearly with decreasing surfactant concentration. This suggests that for all described samples approximately the same absolute amount of surfactant molecules per surface area is involved in the interfacial interactions. This agrees well with an earlier observation that the mesopore diameter in a thin silica film

Table 1. Results of BET Analysis, Mesopore Characterization (BJH calculation), and Micropore Analysis (t-plot) Obtained from the Measured N₂ Adsorption/Desorption Isotherm, Varying Silane to Surfactant Ratios

wt ratio silanes/surfactant ^a	BET surface area (m ² g ⁻¹)	mesopore diameter (nm)	mesopore volume (cm ³ g ⁻¹)	micropore volume (cm ³ g ⁻¹)
2.2	692	9.5	0.56	0.18
7.6	641	22.3	0.54	0.20
15.3	659	18.9	0.58	0.21
22.8	643	17.8	0.54	0.20
30.4	640	13.5	0.50	0.18

^a Silane mixture contains TES40, AAMS, and PTMS and the surfactant is Pluronic 25R4.

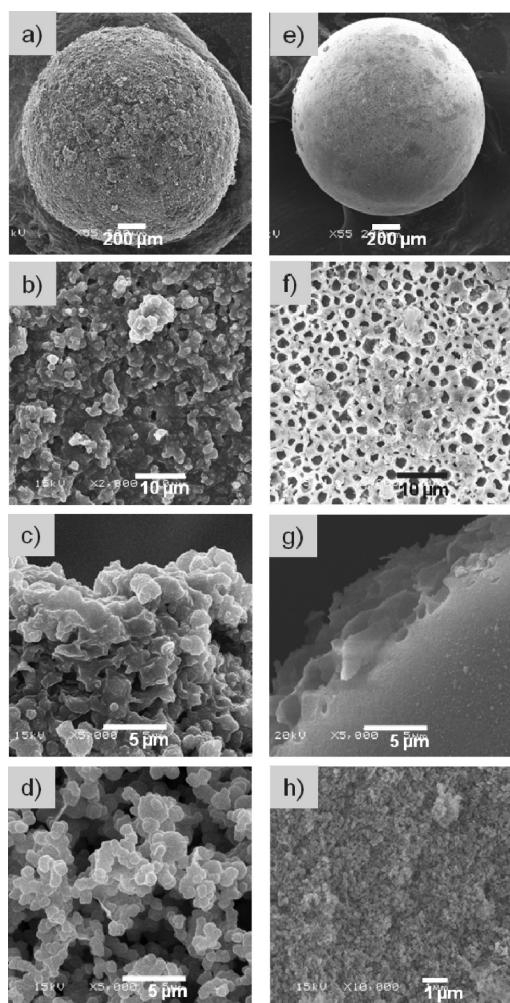


Figure 4. SEM images showing the differences between silica spheres made with (a–d) 1-butanol or (e–h) aniline as solvent. (a, e) Whole sphere, (b, f) surface of the sphere, (c, g) edge of the cross-section, (d, h) center of cross-section.

decreased with decreasing concentration of Brij-76.¹⁸ Note that the sample containing the highest amount of the triblock copolymer does not obey this correlation (Figure 3). This is attributed to the extremely high interfacial surface of the water-in-oil microemulsion resulting in a large number of surface macropores (Figure 2). Consequently, the surfactant concentration in the bulk phase, i.e., inside the precursor droplet is markedly reduced, which results in smaller mesopores.

3.2. Influence of the Solvent. The most important role of the solvent is the contribution to the stabilization of the oil/water

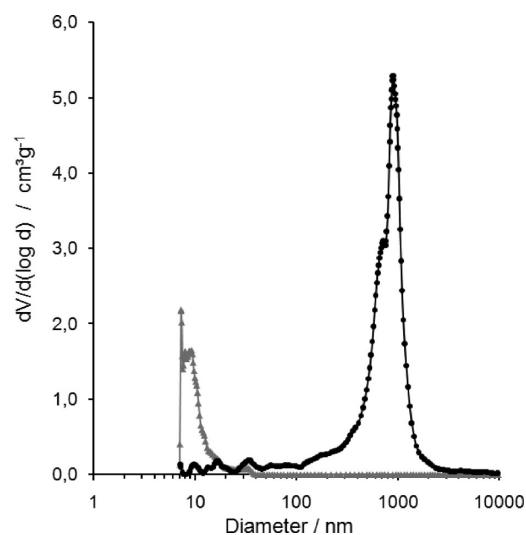


Figure 5. Mercury porosimetry of calcined silica spheres made with aniline (gray line) and 1-butanol (black line) as solvent of the precursor solution.

emulsion by providing a rather low miscibility with water. As preliminary experiments have shown that 1-butanol and aniline exert marked effects on the properties of the final materials, both are systematically explored. 1-Butanol was selected, because alcohols are typically used as solvents to control the hydrolysis and condensation during sol–gel processes. Methanol, ethanol, or propanol typically used in the Stöber process⁴ are not suitable because of their complete miscibility with water. Aniline was chosen as solvent, because it combines basicity and low miscibility with water. Both precursor solutions result in stable droplets and macroscopic silica spheres. While the 1-butanol containing droplets led to opaque white spheres, those prepared with aniline have a transparent milky appearance.

This difference is attributed to variations in the mesoscopic morphology of the spheres, which was analyzed by scanning electron microscopy (Figure 4). The surface of the spheres made with the butanol mixture is rougher and consists of strongly interconnected silica particles. This interconnection between silica particles is reduced from the edge inward leading finally to well-shaped spherical silica particles in the core.

In contrast, the calcined aniline based silica spheres have a macroporous foam-like surface layer, a relatively dense inner shell with hardly distinguishable particles and a fine grained core structure. It should be noticed that the inner part of both samples include particulate structures, while the silica nanoparticles originating from the butanol mixture are approximately ten times larger than the ones originating from an aniline mixture.

In addition to the obvious differences of the morphology, the pore size distribution of these two samples differs as well. The butanol based silica spheres show a high macropore content with a maximum at $\sim 1 \mu\text{m}$. This value agrees well with the estimated size of cavities between the included silica particles. In contrast, the aniline based silica spheres did not form macropores, but only mesopores, which had a diameter of 10 nm, i.e., about 2 orders of magnitude smaller than the pores in materials derived from the 1-butanol based mixture (Figure 5). The mesopore volume of this latter sample is nearly four times higher than that of the macroporous sample. It also had a slightly higher BET surface area and mesopore diameter (Table 2).

The thermogravimetric analysis (Figure 6) shows that the surfactant decomposes at lower temperature ($180 \text{ }^\circ\text{C}$) for the spheres made with 1-butanol than for the ones with aniline ($200 \text{ }^\circ\text{C}$). In addition, the weight loss by surfactant decomposition of the 1-butanol derived spheres occurs rapidly ($180\text{--}200 \text{ }^\circ\text{C}$) and was with 13% less than half of the value determined for the aniline derived sample.

The further decomposition of the organic matter of the two samples occurred nearly in parallel. The weight loss up to $500 \text{ }^\circ\text{C}$ includes the removal of residual carbonaceous species and of the aminosilane, the last step between 500 and $700 \text{ }^\circ\text{C}$ is attributed to the decomposition of phenyltrimethoxysilane.¹⁹ The total weight loss is 53% for the butanol and 61% for the aniline based spheres, which is similar to mesostructured materials such as MCM-41 or SBA-15.¹⁹

Thus, two structured materials differing markedly with respect to the morphology and porosity of the spheres have been prepared by changing the solvent of the precursor solution only.

Table 2. Results of BET analysis, Mesopore Characterization (BJH calculation) and Micropore Analysis (t-plot) Obtained from the Measured N_2 Adsorption/Desorption Isotherm for the Precursor Solutions Containing Aniline and 1-Butanol

	precursor solution with aniline	precursor solution with 1-butanol
surface area ($\text{m}^2 \text{g}^{-1}$)	692	601
mesopore diameter (nm)	9.5	7.1
mesopore volume ($\text{cm}^3 \text{g}^{-1}$)	0.56	0.15
micropore volume ($\text{cm}^3 \text{g}^{-1}$)	0.18	0.25

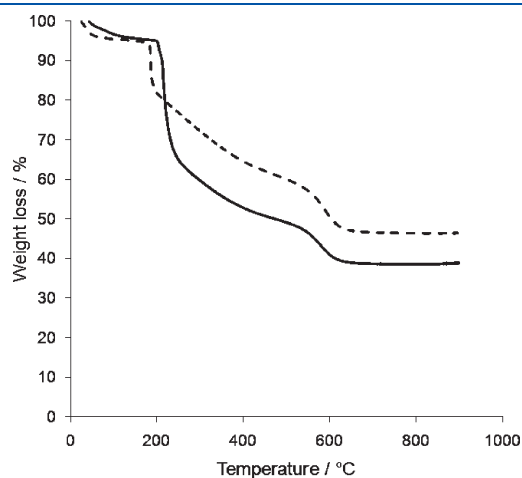


Figure 6. TGA measurement performed on as-made silica composite spheres made with 1-butanol (dashed line) and aniline (solid line).

The main difference between the solvents is the much higher basicity of aniline with a $\text{p}K_b$ value of 9.4. Therefore, aniline contributes to the base catalyzed hydrolysis and condensation of the silanes. In addition, [3-(2-aminoethylamino)propyl]trimethoxysilane acts as catalyst (and constituent) during the sol–gel transition of the precursor solution. Thus, the particulate structure inside the macroscopic silica spheres is attributed to the high pH value during the condensation reaction. The alkaline catalyzed sol–gel process of silicon alkoxides results in a highly branched siloxane network with particulate structure, whereas under acidic conditions more linear and interconnected polysiloxanes are formed.^{4,17,20}

The higher reaction rate by the use of aniline as solvent led to the formation of a large number of primary silica nanoparticles and suppressed so the growth of the single particles. The sol–gel process of butanol containing precursor droplets, in contrast, is only catalyzed by the basic sites of the aminosilane. In addition, the hydrolysis rate of the silanes is decreased by exchange reactions of the more reactive methoxy or ethoxy with butoxy groups.²⁰ Thus, the differences in the morphology are the direct consequence of the lower hydrolysis rate using butanol as solvent, resulting in a smaller initial number of primary silica nanoparticles that subsequently grow due to the reaction with residual silanes. The lower reaction rate in the butanol mixture induces phase separation into a solvent-rich phase and an organosilica phase.^{21,22} Thus, the porosity of the spheres is not only determined by microphase separation due to self-assembly of surfactant molecules, but also by the reaction rate that influences polymerization-induced phase separation.

The amount of surfactant, which is dissolved in the separated butanol phase, is not available for the mesopore formation. The additional loss of the surfactant is also caused by the better solubility of butanol in water showing with 90 g/L more than twice the solubility of aniline. Therefore, a significant amount of the surfactant, which is solved in butanol, will transfer into the water phase. This should lead to a lower concentration of the surfactant in the as-made silica spheres, which has been experimentally verified by thermogravimetry and elementary analysis.

3.3. Variation in the Silane Mixture. The silanes, which were selected for the precursor solution to prepare macroscopic silica spheres, combine three different functions. Tetraethyl silicate is the network building compound to provide stable silica spheres by a three-dimensional connectivity of the SiO_4 tetrahedra. The hydrolysis and condensation of the silanes is autocatalyzed by the basic [3-(2-aminoethylamino)propyl]trimethoxysilane. This prevents the dissolution of the base into the water phase via anchoring to the silica network. Phenyltrimethoxysilane was added to increase the hydrophobicity of the precursor solution for a better phase separation.

Although it is straightforward to accept that the presence of basic functional groups will change the rate of hydrolysis and condensation, the structure and properties of the silica spheres can also be adjusted by the choice of the precursor solution, e.g., by methoxy- and ethoxysilanes, additional basicity by secondary amines, steric demanding functional groups and branched silanes. In specific, we explored different phenyl- and cyclohexylaminosilanes, while keeping the other components such as TES40, AAMS, Pluronic 25R4 as well as aniline constant. All precursor mixtures allowed the preparation of silica composite spheres, i.e., the mixtures formed stable droplets in contact with water and had a sufficiently high reaction rate to prevent agglomeration of the silica spheres.

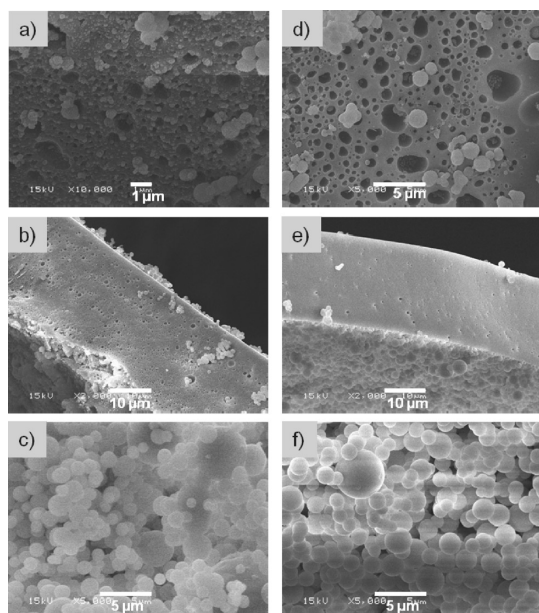


Figure 7. SEM images of calcined silica spheres made with (a–c) XL926 and (d–f) XL924. (a, d) Surface of the spheres, (b, e) edge of the cross-section, (c, f) center of the cross-section.

After calcination, however, some of the spheres made with the ethoxysilanes XL926 and XL924 were cracked and their mechanical stability was much lower than that of the other materials. The reason for this relatively low mechanical stability is attributed to the structure of the spheres (see Figure 7). The hemispheres of split samples of the two materials readily fragmented into the shell and the core. The shell seems to be dense silica, but a closer look reveals numerous macropores with a diameter of 80–540 nm especially for the sample made with XL926 (Figure 7). In contrast, the core consists of large and regular silica particles, which are hardly connected. The size distribution of the silica particles prepared with the monofunctional silane XL926 is broader and slightly shifted to smaller particle sizes compared to the spheres made with the branched silane (XL924).

The spheres prepared with methoxysilanes (instead of ethoxysilanes) are also divided in a core and shell, but these spheres do not break at this interface, indicating a firm connection between the two parts. It is interesting to note that even the nanoparticles of the core are intergrown, which is attributed to the higher reactivity of the methoxy compared to the ethoxy groups. With the more basic silane GF92, the hydrolysis reaction was accelerated, leading to drastically smaller particles in the core (see Figure 8c, f). In addition, the extremely thin shell of these spheres consists of well-ordered macropores with a diameter of approximately 0.8 μm (see Figure 9). The regular distance between the macropores indicates an interaction of the sterically demanding organic group (i.e., the N-cyclohexyl-3-aminopropyl group) with the macropore forming water-filled micelles.

Decreasing the reaction rate of the precursor solution through the usage of ethoxysilanes or silanes with bulky organic functionalities allows the synthesis of spheres with a macroporous shell of controlled thickness between 20 and 26 μm. This shell hinders the water diffusion, which results in a particulate structured core by decreasing the reaction rate through limiting the availability of water. Remarkably, the silane GF92 containing the longest

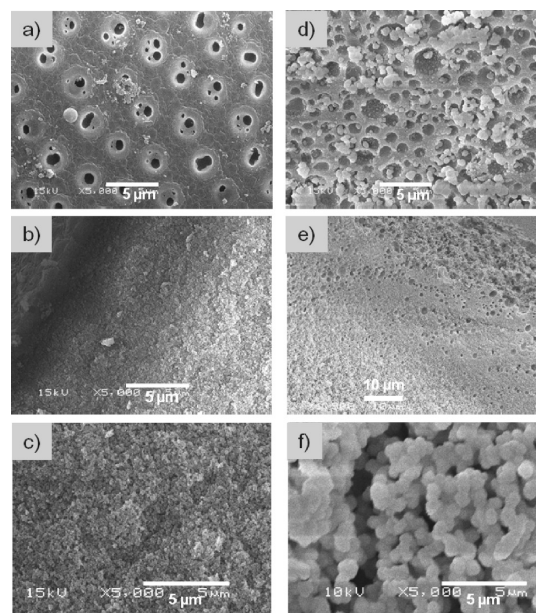


Figure 8. SEM images of calcined silica spheres made with (a–c) GF92 and (d–f) XL973. (a, d) Surface of the spheres, (b, e) edge of the cross-section, (c, f) center of the cross-section.

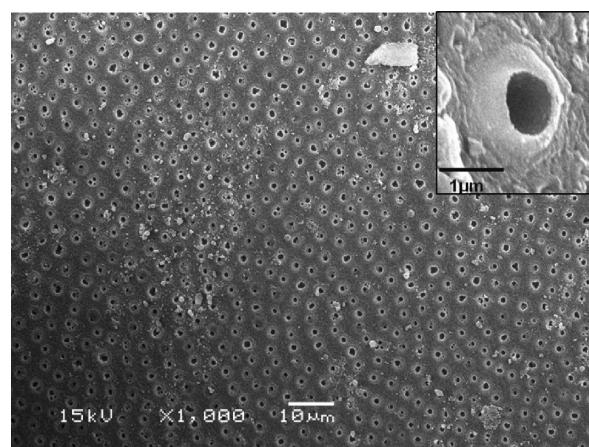


Figure 9. SEM image showing the ordered arrangement of the macropores on the surface of the calcined silica spheres made with GF92 and the magnification of a single pore as an inset.

organic chain induced an ultrathin ordered surface macroporous layer. Despite the steric hindrance, the precursor mixture with GF92 offers a similar reactivity related to PTMS, because of the distinct base site by the secondary amino group. In contrast, the methoxysilane XL973 does not increase the rate of the base catalyzed hydrolysis and condensation, because the secondary amino group is stabilized via the aromatic ring.

The structural differences between the ethoxy- and methoxy based spheres, especially their density, affect the decomposition of the enclosed organic fractions. For the spheres with the lower packing density of the core, the surfactant decomposes more rapidly and at lower temperatures (160 °C) as for the spheres prepared with the methoxysilanes XL973 and GF92 (see Figure 10). It should be noticed that the decomposition step between 500 and 700 °C, which was observed for the sample containing phenyltrimethoxysilane, is missing. This means that in principle lower calcination

temperatures could be applied for the samples with the functional silanes instead of phenyltrimethoxysilane.

With the proper choice of the silane composition, the BET surface area reached values as high as 900 m²/g and the median mesopore diameter varied between 3.8 and 20.6 nm (see Table 3). Overall, the mesopore diameter increased with increasing steric demand of the organic group, which is bound to the trimethoxysilane. This is attributed to the interaction of the organic groups with the self-assembling surfactant molecules increasing so the size of the aggregate. It should be noted, however, that the ethoxysilanes XL926 and XL924 had a very low mesopore diameter and volume, which is attributed to a phase separation induced by the particular silanes. For these two ethoxysilanes, the hydrolysis rate is significantly lower than that of methoxysilanes, which allows the separation in a silane-rich and a solvent-rich phase. Especially if the interactions between the surfactant and the silanes are weak, the template surfactant dissolves better in the solvent-rich phase and hence, is not available for forming pores.

In summary, the variation of the silanes shows a wide variety of possibilities to tune the morphology as well as the porosity of the spheres. The only limitation in this case is a sufficient reaction rate, which can be controlled by the reactivity of the silanes, the addition of a catalyst or the water diffusion influenced by the type of surfactant.

3.4. Extraction of the Surfactant. The question arises, whether or not it is possible to use the organofunctionalized materials without calcination. For this, we extracted the formed spheres with ethanol for 24 and 48 h in a Soxhlet apparatus. During extraction of

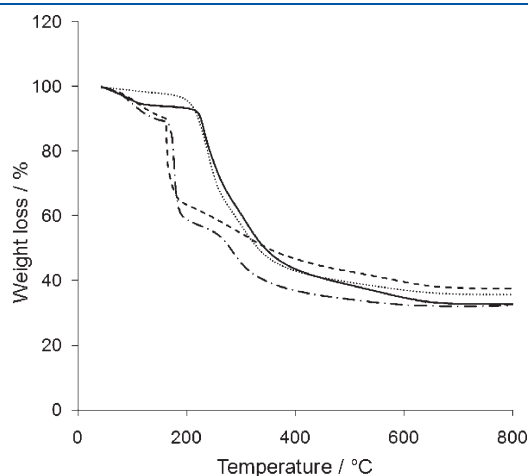


Figure 10. TGA measurement performed on as-synthesized silica composite spheres made with XL973 (dotted line), GF92 (solid line), XL926 (dashed line), and XL924 (dotted-dash line).

the surfactant neither the macroscopic shape nor the structure of the spheres changed significantly. The concentration of C, H and N of the as-prepared sample were 40.5, 5.5, and 3.1 wt %, respectively. After extraction these values decreased to 29.5 wt % carbon, 3.75 wt % hydrogen, and 3.75 wt % nitrogen.

These values are only slightly lower than the expected surfactant concentrations. This is attributed to the fact that the aminosilane AAMS is partly leached from the silica network. Because of protonation of the amino group, the water solubility is significantly increased. The thermogravimetric analysis indicates a small weight loss between 200 and 500 °C, which is a result of the decomposition of residual surfactant and the aminosilane (Figure 11). Compared to the as-synthesized silica spheres, more than 70% of the surfactant was extracted.

3.5. Influence of the synthesis parameters on the materials properties. The properties of the synthesized (organo) silica spheres result mainly from the balance between the hydrolysis and condensation rate and the water diffusion into and inside the precursor droplet, which is strongly influenced by the composition of the precursor solution (Figure 12).

The triblock copolymer acts as surfactant by stabilizing the precursor droplet and enhancing the water transport inside the droplet, as well as a template leading to a controlled mesopore formation. Therefore, the mesopore diameter, the macropore size and arrangement and the surface area depend strongly on the hydrophobicity of the triblock copolymer. The mesopore size can be also controlled by adding different organofunctionalized silanes, whereas the diameter increases with the steric demand of the organo-methoxysilanes. In order

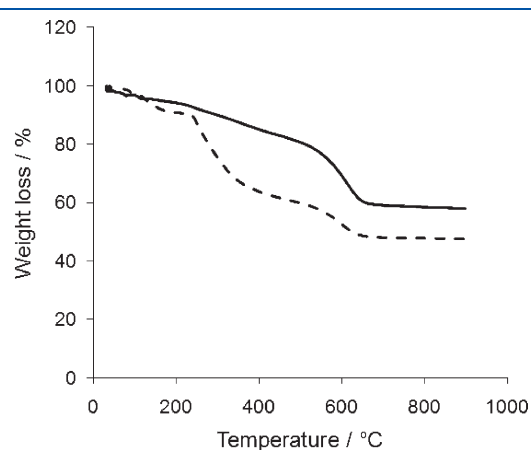


Figure 11. TGA measurement performed on as-synthesized silica composite spheres (dashed line) compared to extracted silica spheres (solid line) containing TES40, AAMS, PTMS, Pluronic RPE1740 and aniline.

Table 3. Results of BET Analysis, Mesopore Characterization (BJH calculation) and Micropore Analysis (t-plot) Obtained from the Measured N₂ Adsorption/Desorption Isotherm, Showing the Influence of Silane Variation

silanes ^a	BET surface area (m ² g ⁻¹)	mesopore diameter (nm)	mesopore volume (cm ³ g ⁻¹)	micropore volume (cm ³ g ⁻¹)
GF92	675	20.6	0.22	0.12
XL973	888	12.1	0.20	0.14
PTMS	692	9.5	0.56	0.18
XL926	713	3.8	0.06	0.14
XL924	636	3.8	0.03	0.10

^aSilane mixture contains TES40, AAMS, and variable silane listed in the table.

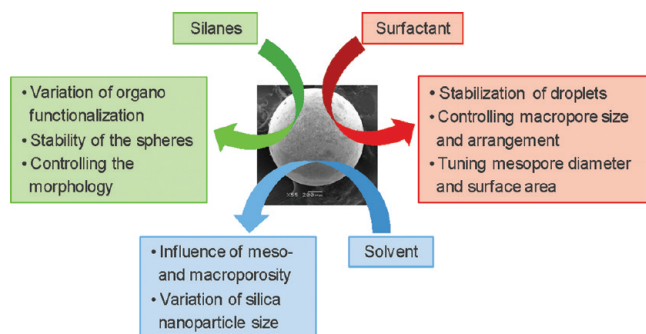


Figure 12. Summary of the main synthesis parameters in correlation to the materials properties.

to tailor the hierarchical core–shell structure of the spheres, the texture of the core, namely the size of the silica nanoparticles depends mainly on the hydrolysis and condensation rate whereas the thickness and porosity of the shell can be adjusted by the hydrophobicity of the precursor solution. The reactivity of the precursor solution and thus the core structure is determined by the solvent and the silane mixture and the hydrophobicity of the precursor droplet can be tuned by the composition of the surfactant molecule as well as by the organic groups of the functional silanes.

4. CONCLUSION

Tailored macroscopic (organo)silica spheres have been prepared in a one-step synthesis by varying the surfactant concentration, the silane mixture, the solvent as well as the method to remove structure directing agents as key parameters to design the materials. Overall, the morphology and the properties of the spheres are controlled by the combination of phase separation and sol–gel transition. The key is to understand not only the chemistry induced by each component but also their mutual influence.

The hierarchical structure is mainly controlled by the reactivity of the precursor solution and the rate of water diffusion into the sphere after initial (macroscopic) phase separation. The precursor droplets are stabilized by the alignment of surfactant molecules along the oil–water interface and the water diffusion inside the droplet occurs by the formation of a water-in-oil microemulsion. Thus, the macro- and microstructure of the silica spheres is strongly influenced by the surfactant concentration. The well ordered macroporous shell, which is formed from the microemulsion, is detected for high surfactant concentrations, whereas decreasing the concentration results in a less-ordered surface structure as well as less-stabilized droplets and smaller mesopores.

The solidification of the precursor droplets proceeds via base-catalyzed sol–gel reactions. Hence, the usage of aniline as solvent is advantageous, because it acts in a dual function providing hydrophobicity to stabilize the droplet and basicity to catalyze the sol–gel reaction resulting in mechanically stable, mesoporous silica spheres. Reducing the reaction rate by changing the solvent or the silane mixture allows the preparation of macroporous silica spheres.

The mesoporosity, however, is not only controlled by the choice of surfactant, but also by the modification of the organofunctionalized silanes in the precursor solution. The interaction of steric demanding organic groups with the self-assembled surfactant aggregates leads to an increased mesopore diameter.

Especially large functional groups, such as the cyclohexylamino-propyl moiety of GF92, are able to direct the self-assembling surfactant molecules in order to create regular macropores on the surface of the spheres. Co-condensation of a network building compound with the organofunctionalized silanes allows in turn the synthesis of hybrid organo-silica spheres when structure directing components are removed by solvent extraction.

■ ASSOCIATED CONTENT

S Supporting Information. The technical drawing of the reactor column and a schematic representation of the preparation principle. This material is available free of charge via the Internet at <http://pubs.acs.org>

■ AUTHOR INFORMATION

Corresponding Author

*E-mail: johannes.lercher@ch.tum.de. Tel.: 089/28913540. Fax: 089/28913544.

■ ACKNOWLEDGMENT

Financial support by Wacker Chemie AG and fruitful discussions within the Wacker-Institut für Siliciumchemie and the framework of the network of excellence IDECAT is gratefully acknowledged. The authors thank Wacker Chemie AG and the BASF Corporation for the gift of the Geniosil silanes, TES40, and the Pluronic polymers, Dipl.-Ing. Martin Neukamm for SEM analysis, Dipl.-Ing. Xaver Hecht for BET analysis and Hg-porosimetry, Georgeta Krutsch and Aleksandra Jonovic for TGA measurements, Ulrike Ammari and co-workers from the microanalytical lab for elementary analysis, and Dr. Yongzhong Zhu for helpful discussions.

■ REFERENCES

- (1) Schlögl, R.; Abd Hamid, S. B. *Angew. Chem., Int. Ed.* **2004**, *43*, 1628.
- (2) Schacht, S.; Huo, Q.; Voigt-Martin, I. G.; Stucky, G. D.; Schüth, F. *Science* **1996**, *273*, 768.
- (3) Grün, M.; Lauer, I.; Unger, K. K. *Adv. Mater.* **1997**, *9*, 254.
- (4) Stöber, W.; Fink, A.; Bohn, E. *J. Colloid Interface Sci.* **1968**, *26*, 62.
- (5) Alonso, B.; Douy, A.; Veron, E.; Perez, J.; Rager, M. N.; Massiot, D. *J. Mater. Chem.* **2004**, *14*, 2006.
- (6) Huo, Q. S.; Feng, J. L.; Schüth, F.; Stucky, G. D. *Chem. Mater.* **1997**, *9*, 14.
- (7) Yuan, Z. Y.; Su, B. L. *J. Mater. Chem.* **2006**, *16*, 663.
- (8) Sen, T.; Tiddy, G. J. T.; Cascic, J. L.; Anderson, M. W. *Chem. Commun.* **2003**, 2182.
- (9) Carn, F.; Colin, A.; Achard, M. F.; Deleuze, H.; Sellier, E.; Birot, M.; Backov, R. *J. Mater. Chem.* **2004**, *14*, 1370.
- (10) Oh, C.; Chung, S. C.; Shin, S. I.; Kim, Y. C.; Im, S. S.; Oh, S. G. *J. Colloid Interface Sci.* **2002**, *254*, 79.
- (11) Witossek, H.; Bratz, E. *Chem. Eng. Technol.* **1997**, *20*, 429.
- (12) Landfester, K. *Annu. Rev. Mater. Res.* **2006**, *36*, 231.
- (13) Mann, S.; Burkett, S. L.; Davis, S. A.; Fowler, C. E.; Mendelson, N. H.; Sims, S. D.; Walsh, D.; Whilton, N. T. *Chem. Mater.* **1997**, *9*, 2300.
- (14) Zhao, D. Y.; Huo, Q. S.; Feng, J. L.; Chmelka, B. F.; Stucky, G. D. *J. Am. Chem. Soc.* **1998**, *120*, 6024.
- (15) Beck, J. S.; Vartuli, J. C.; Roth, W. J.; Leonowicz, M. E.; Kresge, C. T.; Schmitt, K. D.; Chu, C. T. W.; Olson, D. H.; Sheppard, E. W.; McCullen, S. B.; Higgins, J. B.; Schlenker, J. L. *J. Am. Chem. Soc.* **1992**, *114*, 10834.

- (16) Huo, Q. S.; Margolese, D. I.; Ciesla, U.; Feng, P. Y.; Gier, T. E.; Sieger, P.; Leon, R.; Petroff, P. M.; Schüth, F.; Stucky, G. D. *Nature* **1994**, *368*, 317.
- (17) Zhao, D. Y.; Feng, J. L.; Huo, Q. S.; Melosh, N.; Fredrickson, G. H.; Chmelka, B. F.; Stucky, G. D. *Science* **1998**, *279*, 548.
- (18) Jung, S. B.; Park, H. H. *Thin Solid Films* **2006**, *494*, 320.
- (19) Kleitz, F.; Schmidt, W.; Schüth, F. *Microporous Mesoporous Mater.* **2003**, *65*, 1.
- (20) Iler, R. K. *The Chemistry of Silica*; John Wiley & Sons: New York, 1979.
- (21) Schiller, R.; Weiss, C. K.; Geserick, J.; Hüsing, N.; Landfester, K. *Chem. Mater.* **2009**, *21*, 5088.
- (22) Nakanishi, K. J. *Porous Mater.* **1997**, *4*, 67.